

Turn down genes for WAT? Activation of anti-apoptosis pathways protects white adipose tissue in metabolically depressed thirteen-lined ground squirrels

Samantha M. Logan¹ · Bryan E. Luu¹ · Kenneth B. Storey¹

Received: 9 November 2015 / Accepted: 25 March 2016 / Published online: 31 March 2016
© Springer Science+Business Media New York 2016

Abstract During hibernation, the metabolic rate of thirteen-lined ground squirrels (*Ictidomys tridecemlineatus*) can drop to <5 % of normal resting rate at 37 °C, core body temperature can decrease to as low as 1–5 °C, and heart rate can fall from 350–400 to 5–10 bpm. Energy saved by hibernating allows squirrels to survive the winter when food is scarce, and living off lipid reserves in white adipose tissue (WAT) is crucial. While hibernating, some energy must be used to cope with conditions that would normally be damaging for mammals (e.g., low core body temperatures, ischemia) and could induce cell death via apoptosis. Cell survival is largely dependent on the relative amounts and activities of pro- and anti-apoptotic Bcl-2 family proteins. The present study analyzed how anti-apoptotic proteins respond to protect WAT cells during hibernation. Relative levels of several anti-apoptotic proteins were quantified in WAT via immunoblotting over six time points of the torpor-arousal cycle. These included anti-apoptotic Bcl-2 family members Bcl-2, Bcl-xL, and Mcl-1, as well as caspase inhibitors x-IAP and c-IAP. Changes in the relative protein levels and/or phosphorylation levels were also observed for various regulators of apoptosis (p-JAKs, p-STATs, SOCS, and PIAS). Mcl-1 and x-IAP protein levels increased whereas Bcl-xL, Bcl-2, and c-IAP protein/phosphorylation levels decreased signifying important roles for certain Bcl-2 family members in cell survival over the torpor-arousal cycle. Importantly, the relative phosphorylation of selected STAT proteins

increased, suggesting a mechanism for Bcl-2 family activation. These results suggest that an increase in WAT cytoprotective mechanisms supports survival efforts during hibernation.

Keywords White adipose tissue · Apoptosis · Bcl-2 family · Thirteen-lined ground squirrel · Torpor-arousal cycle · JAK–STAT

Introduction

Hibernation is the energy-saving mechanism that allows many small mammals to survive harsh winter conditions consisting of low temperatures and little or no food availability [1]. The thirteen-lined ground squirrel (*Ictidomys tridecemlineatus*) is a well-studied model hibernator. These animals undergo numerous torpor-arousal cycles each winter season where their metabolic rate can drop as low as 1–5 % of the normal resting rate at 37 °C and body temperature can range from normal euthermic values of 36–37 °C to as low as about 5 °C during torpor [1]. All physiological parameters are suppressed: e.g., breathing rate can decrease to just 2.5 % of normal, heart rate can fall from 350–400 to 5–10 bpm, and organ perfusion rate can also decrease to <10 % of the euthermic level [2, 3]. Non-hibernating mammals exposed to extreme cold need to greatly increase heat production and conservation, which is an energetically expensive process that can lead to exhaustion, hypothermia, and death [4]. By entering hibernation, ground squirrels save nearly 90 % of the energy that they would otherwise need to maintain a body temperature of 37 °C over the winter season [3]. During the late summer months, ground squirrels prepare for hibernation by going through a period of hyperphagia—extreme

✉ Kenneth B. Storey
kenneth_storey@carleton.ca

¹ Institute of Biochemistry and Department of Biology,
Carleton University, 1125 Colonel By Drive, Ottawa,
ON K1S 5B6, Canada

eating where animals gain up to 50 % of their starting weight, mostly as lipids stored in white adipose depots [5]. Enzymatic adjustments are made so that all organs favor the use of lipid catabolism for energy production during torpor. This includes the brain which derives much of its winter energy from the oxidation of ketone bodies made from fatty acids in the liver [2]. White adipose tissue (WAT), which is present subcutaneously and in the abdomen, is the crucial lipid storage organ that supplies the fatty acid fuels for lipid catabolism. WAT is susceptible to apoptosis caused by local hypoxia, high sucrose, and saturated fat diets, as well as changes in hormone, antioxidant, and linoleic acid levels [6–8]. Thus, it is essential to preserve the integrity of WAT in order to ensure mammalian survival during hibernation.

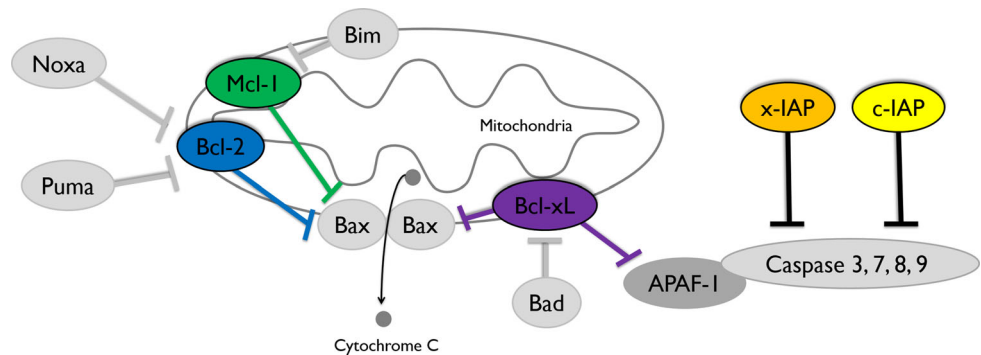
Apoptosis is a mode of cell death where infected, damaged, or unwanted cells are destroyed from within so as to not disrupt healthy, neighboring cells [9]. Intrinsic cellular signals from events such as nutrient deprivation, hypoxia, DNA damage, ion imbalances, etc., as well as extrinsic cellular signals from the presence of cytokines, steroids, toxins, etc., can promote or accelerate apoptosis [10]. Whether a cell will live or die is dependent on the relative amounts and activities of the pro- and anti-apoptotic B cell lymphoma (Bcl-2) family of proteins that respond to these intrinsic and extrinsic signals [11]. The most common form of apoptosis used by vertebrates is the intrinsic mitochondrial pathway, where cellular stress signals lead to the activation of pro-apoptotic Bcl-2 family members (BIM, PUMA, tBID, NOXA, etc.) and their binding to anti-apoptotic Bcl-2 family members (Bcl-2, Mcl-1, Bcl-xL, etc.), resulting in pro-apoptotic BAK and BAX release and oligomerization [10, 11]. BAK and BAX induce pore formation in the mitochondria, termed “mitochondrial outer membrane permeabilization” (MOMP), which leads to the release of pro-apoptotic molecules (like cytochrome c) from between the mitochondrial inner and outer membranes. Cytochrome c promotes the ATP-dependent oligomerization of apoptotic protease activating factor-1 (APAF-1) to form the caspase-9-activating “apoptosome” [10, 11]. Activated caspase-9 is able to cleave caspase-3 and caspase-7 proforms, resulting in active “effector” proteases that cleave cellular contents for disposal [10]. An alternate way to activate caspases is via the extrinsic apoptotic pathway, activated extracellularly by the docking of ligands from a neighboring cell to death receptors of the cell targeted for destruction [12]. Activated by this stimulus, caspase-8 activates caspase-3 to initiate the destruction of the cell’s contents [12]. Irreversible cellular demolition initiated by the intrinsic apoptotic pathway occurs only when there is an imbalance of pro- and anti-apoptotic proteins, in the favor of cell death [11]. The core pro-survival (anti-apoptotic) Bcl-2 family

members involved in the inhibition of MOMP in the intrinsic apoptotic pathway include Bcl-2, Bcl-xL, and Mcl-1 [13]. An additional level of apoptosis regulation occurs downstream of the mitochondria: pro-survival inhibitor of apoptosis proteins (IAPs), x-IAP, and c-IAP1/2, are able to inhibit caspases activated by both the intrinsic and the extrinsic apoptotic pathways, including caspases-3, -7, -8, and -9 (Fig. 1) [14, 15].

The Janus kinase–signal transducer and activator of transcription (JAK–STAT) pathway is an important signal transduction pathway that is active in cells under stress, especially in tissues where there is a battle between cell survival and apoptosis [16–18]. Phosphorylation of key STAT tyrosine residues is correlated with STAT localization to the nucleus and altered gene transcription [19, 20]. Conversely, STATs are largely dephosphorylated in the cytoplasm. Once dissociated from the regulatory JAKs, STAT proteins can homodimerize or heterodimerize and translocate to the nucleus where they bind palindromic TTC(N)_{3–4}GAA consensus sequences to initiate transcription of target genes [19, 21, 22]. Seven STAT members have been identified in mammals, each known to regulate different processes [23]. For example, STAT1 has been found to promote cell death in neural and cardiac tissue following ischemia–reperfusion, in human fibroblast cells following actinomycin D and TNF- α exposure, and in rat liver cells following hypothermia [18, 24]. In contrast, STAT3 is capable of upregulating Mcl-1, Bcl-2, Survivin, and Bcl-xL expression to promote cell survival [16, 17, 25]. Protein inhibitors of activated STATs (PIAS) and suppressors of cytokine signaling (SOCS) are two of the three main regulators of JAK–STAT activity. PIAS proteins inhibit STAT activity by blocking DNA binding or by recruiting co-repressors, whereas SOCS proteins inhibit JAK-mediated phosphorylation and activation of STATs [20, 26–28].

The study of apoptotic pathways in hibernating mammals can reveal how tissue damage and cell survival is controlled despite the dramatic physiological and biochemical changes that these animals experience over repeated bouts of torpor-arousal and under severe winter environmental conditions. A recent study provided evidence for a potential role of anti-apoptotic proteins in the heart and brain of thirteen-lined ground squirrels during torpor [29]. The present study explores the regulation of key controllers of apoptosis in thirteen-lined ground squirrel white adipose tissue throughout the torpor-arousal cycle. Relative protein expression of Bcl-2, Bcl-xL, Mcl-1, x-IAP, and c-IAP1/2 were assessed by immunoblotting. Furthermore, immunoblotting was also used to assess relative phosphorylation levels of p-Bcl-2 (S70), p-Bcl-2 (T56), p-Bcl-xL (S62), and p-Mcl-1 (S159) in ground squirrel white adipose tissue over the torpor-arousal cycle.

Fig. 1 Anti-apoptotic proteins at the mitochondrial membrane. Anti-apoptotic proteins of interest are displayed in *color*. Pro-apoptotic proteins are displayed in *gray scale*. Adapted and modified from Rouble et al. [29]



Luminex analysis measured the relative phosphorylation levels of p-STAT1 (Y701), p-STAT2 (Y690), and p-STAT3 (Y705). Lastly, immunoblotting was also employed to measure relative levels of protein expression and phosphorylation for upstream regulators of anti-apoptosis, namely p-JAK1 (Y1022/1023), p-JAK2 (Y1007/1008), p-JAK3 (Y908), SOCS1-3, and PIAS1/3. In general, it was found that the levels of anti-apoptotic proteins increased when squirrels entered torpor whereas the relative phosphorylation of these proteins generally decreased, signifying that cell survival mechanisms are enhanced during torpor in one of the most important tissues in the hibernating ground squirrel.

Materials and methods

Animals

Thirteen-lined ground squirrels (*Ictidomys tridecemlineatus*) weighing approximately 150–300 g, were wild captured by a United States Department of Agriculture-licensed trapper (TLS Research, Bloomingdale, IL) and transported to the laboratory of Dr. J.M. Hallenback at the Animal Hibernation Facility, National Institute of Neurological Disorders and Stroke (NINDS) (NIH, Bethesda, MD) where the hibernation experiments were conducted. Animal housing and experimental procedures were approved by the NINDS animal care and use committee (ACUC). Each thirteen-lined ground squirrel was fitted with a sensor chip (IPTT-300; Bio Medic Data Systems) injected subcutaneously while anesthetized with 5 % isoflurane and was housed individually in a shoebox cage at 21 °C. Animals were fed a standard rodent diet and water ad libitum until they gained sufficient lipid stores to enter hibernation. To enable a natural transition into torpor, animals were transferred to an environmental chamber at ~5 °C in constant darkness. Body temperature (T_b), time, and respiration rate were observed to determine sampling points. All thirteen-lined ground squirrels had been through

torpor-arousal bouts prior to sampling and were sampled as previously described [30]. Tissue samples were shipped to Carleton University on dry ice. The tissues were stored at –80 °C until use. EC designates euthermic, cold room; these euthermic animals had a stable T_b (~37 °C) in the 5 °C cold room, were able to enter torpor but had not done so for at least 3 days. EN designates entrance; animals were in the entrance phase of the hibernation bout characterized by decreasing T_b and were sampled when T_b was 18–31 °C. ET designates early torpor; animals had a stable T_b of 5–8 °C for 1 day. LT designates late torpor; animals that were continuously in deep torpor for at least 5 days with T_b values of 5–8 °C. EA designates early arousal animals characterized by an increased respiratory rate of >60 breaths/min and a rising T_b of 9–12 °C. IA designates interbout arousal after a multi-day torpor with core body temperature returned to ~37 °C for approximately 18 h.

Protein extraction for western blotting

Total protein extracts ($n = 4$ independent biological replicates) of white adipose tissue (WAT) were prepared for 6 time points (EC, EN, ET, LT, EA, and IA) as previously described [31]. Frozen samples were quickly weighed and then crushed into small pieces under liquid nitrogen. The tissue was homogenized 1:3 w:v with a Polytron P10 homogenizer in ice-cold homogenizing buffer (20 mM HEPES, 200 mM NaCl, 0.1 mM EDTA, 10 mM NaF, 1 mM Na_3VO_4 , and 10 mM β -glycerophosphate, pH 7–8), along with a few crystals of PMSF and 1 $\mu\text{L}/\text{mL}$ of protease inhibitor cocktail (Sigma). Homogenates were centrifuged at 10,000 rpm for 10 min at 4 °C, supernatants were retained, and total soluble protein concentration was determined using the Bio-Rad protein reagent (Bio-Rad; Hercules, CA). Protein concentrations of the samples were adjusted to a constant 10 $\mu\text{g}/\mu\text{L}$ by adding appropriate small volumes of homogenizing buffer. Aliquots were then mixed 1:1 v:v with 2 \times SDS loading buffer (100 mM Tris-base, pH 6.8, 4 % w:v SDS, 20 % v:v glycerol, 0.2 % w:v

bromophenol blue, 10 % v:v 2-mercaptoethanol), then vortexed, boiled for 5 min, and stored at -40 °C until use.

Protein extraction for Luminex® assay

Protein extracts were prepared from frozen tissue samples according to the manufacturer's instructions and as previously described [32]. Briefly, approximately 50 mg of frozen tissue from each of the 6 time points was weighed and immediately homogenized 1:4 w:v with a glass homogenizer in ice-cold lysis buffer (1 mM Na₃VO₄, 10 mM NaF, 10 mM β-glycerophosphate, and 10 μL/mL Sigma protease inhibitor). After incubation on ice for 30 min with occasional vortexing, samples were centrifuged at 10,000 rpm for 20 min at 4 °C. The supernatant of each sample was removed and its protein concentration was determined using the Bio-Rad protein reagent. Samples were diluted to 0.5 μg/μL with Assay Buffer 2 (EMD Millipore; Cat#43-041). Positive and negative controls provided by the manufacturer were used in each assay, and were prepared according to the manufacturer's instructions. For the STAT Phosphoprotein Magnetic Bead Kit (Cat#48-610MAG), unstimulated HeLa cell lysate (Cat#47-205) was used as a negative control, whereas HeLa cell lysate: IFNα (Cat#47-226) and Daudi cell lysate (Cat#47-217) were used as positive controls. For the Human Late Apoptosis Magnetic Bead Kit (Cat#48-670MAG), unstimulated Jurkat cell lysate (Cat#47-206) was used as a negative control, and Jurkat cell lysate: Anisomycin (Cat#47-207) was used as a positive control. The appropriate amount of assay buffer was added to the reconstituted lysates, as described in the manufacturer's instructions.

Western blotting

Equal amounts of protein sample (40 μg/well) were added to 8 % SDS-PAGE gels (for p-JAK1-3 and PIAS1 and 3), to 10 % SDS-PAGE gels (for Mcl-1, x-IAP, and c-IAP), and to 15 % SDS-PAGE gels (for Bcl-xL, p-Bcl-xL (S62), Bcl-2, p-Bcl (T56), p-Bcl-2 (S70), and SOCS1-3). Each gel was then run at 180 V in running buffer (0.25 M Tris-base, 2.45 M glycine, and 0.035 M SDS) for varying amounts of time: 55 min for PIAS1 and 3, 65–70 min for Mcl-1, Bcl-2, p-Bcl-2 (T56), p-Bcl-2 (S70), Bcl-xL, p-Bcl-xL (S62), SOCS1-3, and p-JAK1-3, and 90 min for x-IAP and c-IAP. Proteins were then transferred onto 0.45 μm PVDF membrane by electroblotting at 160 mA in transfer buffer (25 mM Tris pH 8.5, 192 mM glycine, and 10 % v/v methanol) for varying amounts of time at 4 °C: 70 min for SOCS1-3, phospho- and nonphospho-Bcl-2 and Bcl-xL proteins and 90 min for x-IAP, c-IAP, PIAS1, PIAS3, and Mcl-1. Phosphorylated JAK proteins were transferred to PVDF membrane at 4 °C for 150 min. Following one wash with TBST (20 mM Tris-base pH 7.6, 140 mM NaCl, and

0.05 % v:v Tween-20), each membrane was blocked with 1.5 % w:v skim milk in TBST for 15 min. Each membrane was then probed overnight or for 2 days at 4 °C with primary antibody (diluted 1:1000 v:v in TBST). Primary antibodies were purchased from Cell Signaling: Bcl-2 Cat#2870P, Bcl-xL Cat#2764P, p-Bcl-2 (S70) Cat#2827P, p-Bcl-2 (T56) Cat#2875P, Mcl-1 Cat#5453P, SOCS1 Cat#3950P, SOCS2 Cat#2779P, SOCS3 Cat#2932P, PIAS1 Cat#3550P, PIAS3 Cat#4164P. The p-JAK1-3, p-Bcl-xL (S62), and c-IAP1/2 primary antibodies were purchased from Santa Cruz Biotechnology: p-JAK1 (Y1022/1023) Cat#sc-16773-R, p-JAK2 (Y1007/1008) Cat#sc-16566-R, p-JAK3 (Y980) Cat#sc-16567-R, p-Bcl-xL Cat#sc-101644, c-IAP1/2 Cat#sc-12410. The p-Mcl-1 (S159) primary antibody was from GenWay Biotech Inc. (Cat#GWB-ASB518) and the x-IAP primary antibody was from Stressgen (Cat#ALX-210-327-C100). Membranes were then probed with an HRP-linked anti-rabbit IgG secondary antibody (1:3000 v:v in TBST) for 50 min. Following three washes with TBST (10 min/wash), bands were visualized by enhanced chemiluminescence (H₂O₂ and Luminol).

Luminex® assay

A Luminex multiplex panel was used to measure STAT phosphorylation levels and pro-apoptotic target levels in WAT samples (EMD Millipore; STAT Phosphoprotein Magnetic Bead Kit, Cat#48-610MAG and Human Late Apoptosis Magnetic Bead Kit, Cat#48-670MAG). Targets included p-STAT1 (Y701), p-STAT2 (Y690), and p-STAT3 (Y705), PARP (cleaved), and caspase-3 (active). The protocol for each multiplex analysis was performed as instructed by the manufacturer. Briefly, the premixed antibody capture beads that were supplied with each kit (EMD Millipore; Cat#42-610MAG and Cat#42-670MAG) were sonicated, vortexed, and diluted as required. After incubation with assay buffer, sample or control lysates were individually combined with the premixed beads. An overnight incubation on a shaker at 4 °C in the dark was used for the STAT Phosphoprotein Magnetic Bead Kit and a 2 h incubation on a shaker at 4 °C in the dark was used for the Human Late Apoptosis Magnetic Bead Kit. Following incubations, the microplate was placed on a Handheld Magnetic Separator Block (Cat#40-285) for 60 s and the wells were emptied of the lysates. Assay Buffer was used to wash the wells twice. After decanting the assay buffer with the magnetic separation block attached, the Milliplex Map Detection Antibody corresponding to the STAT Phosphoprotein and Late Apoptosis kits (EMD Millipore, Cat#44-610KMG and Cat#44-670KMG, respectively) was vortexed, diluted, and added to each well as described by the manufacturer. The microplate was then sealed, covered, and placed on a rocker to shake for 1 h at room temperature. Subsequently, the wells were decanted, washed, and incubated with

appropriately prepared Streptavidin–Phycoerythrin (EMD Millipore; Cat#45-001H) for 15 min at room temperature on a plate shaker protected from light. Milliplex Map Amplification Buffer (EMD Millipore; Cat#43-024A) was then added to each well and rocked for 15 min at room temperature in the dark. The buffer was then decanted, the beads were resuspended in Assay Buffer, and the microplate rocked at room temperature for 5 min before taking measurements. Median fluorescent intensity (MFI) was collected using a Luminex® 200 instrument and xPonent software (Luminex® Corporation).

Statistics

A Chemi Genius Bioimaging system (Syngene, Frederick, MD) was used to visualize band densities on chemiluminescent immunoblots and GeneTools software was used to quantify band densities. Due to the limited number of samples that can be loaded on every gel, one experimental condition was run on all three gels for each protein target, and used as a standardizing experimental condition for relative quantification. Since the amount of sample was limited, different experimental conditions were used for standardization: EC was run on all three p-JAK1 and p-JAK2 blots, EN was used for p-JAK3, PIAS1, and PIAS3 blots, ET was used for p-Bcl-2 (S70), PIAS4, and SOCS1-3 blots, LT was used for Bcl-2, p-Bcl-2 (T56), Bcl-xL, and Mcl-1 blots, and IA was used for c-IAP, x-IAP, p-Bcl-xL, and p-Mcl-1 blots. The average EC value was arbitrarily assigned to one for graphing purposes and all other relative values of experimental conditions were standardized to this value. Immunoblots were re-stained using Coomassie blue (0.25 % w:v Coomassie brilliant blue, 7.5 % v:v acetic acid, 50 % methanol) to visualize all protein bands. Immunoblot band density in each lane was standardized against the summed intensity of a group of Coomassie-stained protein bands in the same lane. All multiplex MFI values were above those from background wells and were acquired with a minimum bead count of 50. Data are expressed as mean \pm SEM, $n = 4$ independent samples from different animals. Standardized band intensities and MFI values were analyzed with a one-way ANOVA followed by Tukey's post hoc test, where $p < 0.05$ represents a statistically significant difference.

Results

Relative protein and phosphorylation levels of anti-apoptotic targets

Immunoblotting was used to determine the relative total protein levels of Bcl-2, Bcl-xL, Mcl-1, c-IAP, x-IAP and

their relative phosphorylation states in white adipose tissue (WAT) of thirteen-lined ground squirrels, comparing six stages of the torpor-arousal cycle: EC (euthermic animals in the cold room; the control condition), EN (entry into torpor with T_b decreasing), ET (early torpor with a stable low T_b for ~ 1 day), LT (late torpor with a stable low T_b for at least 5 days), EA (early arousal with T_b and respiration rate rising), and IA (interbout arousal with T_b returned to euthermic levels for ~ 18 h) (see more details in the Methods). Total Bcl-2 protein levels fell progressively as animals entered and established torpor dropping to less than 30 % of the EC value during ET, and reaching 14 % of EC during LT. Levels rose again somewhat during EA and IA but remained significantly reduced with respect to EC at 45 and 47 %, respectively (Fig. 2). Relative phosphorylation levels of p-Bcl-2 (T56) followed the same pattern with a significant decrease during EN to about half of the EC value and dropping further to ~ 20 % of the EC value during ET and then to 15 % in LT. Levels rose again during arousal but remained at <50 % of the EC value during EA and IA. By contrast, p-Bcl-2 (S70) levels remained high relative to the EC value throughout, except during LT, when phosphorylation state was strongly reduced to just 20 % of the EC value. Figure 3 shows the analysis of Bcl-xL levels. Two bands were apparent on the total Bcl-xL blot, but only the top band was quantified because it matched the expected molecular weight of the protein and was similar in size compared to the single p-Bcl-xL (S62) band. No changes in relative Bcl-xL protein levels were observed over the torpor-arousal cycle but the relative phosphorylation state of p-Bcl-xL (S62) showed a reduced trend over torpor-arousal with a significant drop to 40 % of the EC value seen during EA.

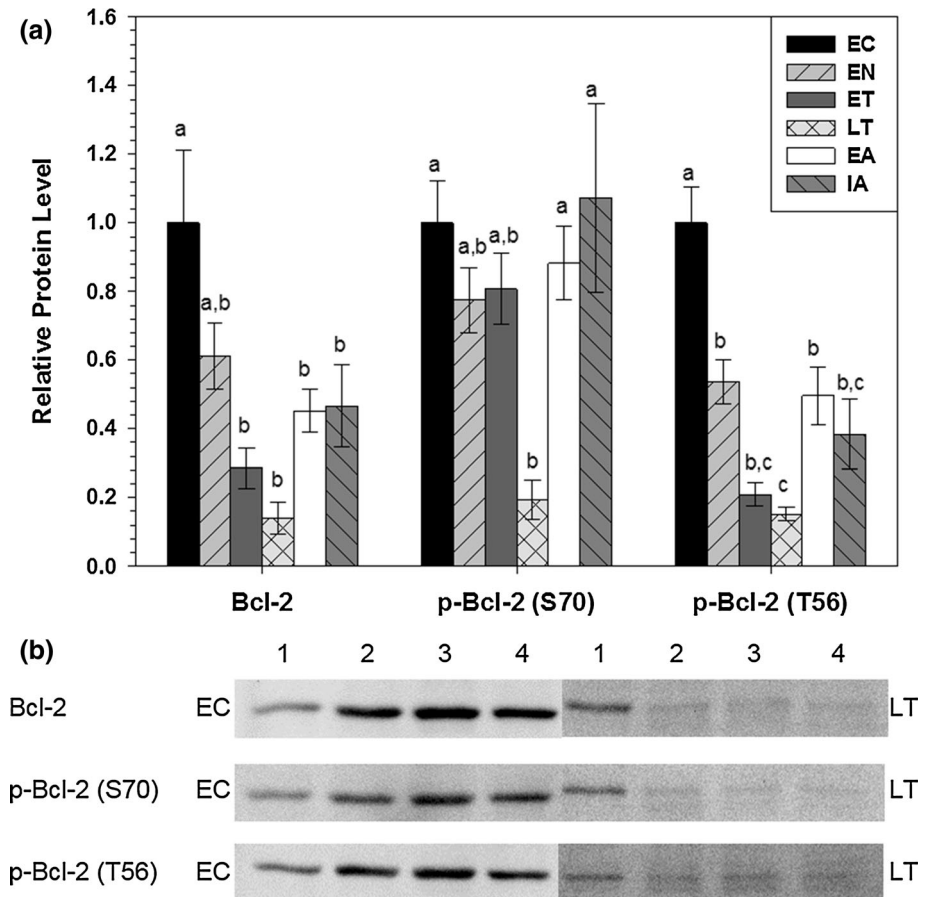
Data for Mcl-1 responses to torpor-arousal are shown in Fig. 4. Compared to EC, Mcl-1 total protein increased by 2.2-fold and 3.1-fold during EA and IA, respectively. Both of these increases were significant with respect to EN and the increase in Mcl-1 during IA was also significant compared to ET and LT. In contrast, relative levels of p-Mcl-1 (S159) declined to 16, 27, 20, 22, and 26 % of the EC level during EN, ET, LT, EA, and IA, respectively (Fig. 4).

Compared to EC levels, total x-IAP protein increased sharply by 13.7-fold during ET and remained elevated at 8–9 fold above EC during LT and EA (Fig. 5). However, X-IAP levels decreased significantly during IA to a level ~ 2.5 -fold higher than the EC value. The levels of c-IAP did not change over the course of the torpor-arousal cycle (Fig. 5).

Relative protein levels of pro-apoptotic targets

The relative levels of poly-(ADP-Ribose) polymerase (PARP) (cleaved) and caspase-3 (active) were determined in WAT, across 6 time points of the torpor-arousal cycle,

Fig. 2 Relative Bcl-2 protein and phosphorylation levels in white adipose tissue (WAT) of thirteen-lined ground squirrels. **a** Histogram showing mean standardized expression levels of Bcl-2, p-Bcl-2 (S70), and p-Bcl-2 (T56) (\pm SEM, $n = 3$ –4 independent protein isolations from different animals, where $n = 3$ was used for p-Bcl-2 (S70) EN, LT, and IA). **b** Representative western blots for EC and LT conditions. Data were analyzed using ANOVA with a Tukey post hoc test. Shared letters indicate data that are not significantly different from each other and different letters indicate statistically significant differences between sample points ($p < 0.05$)



using a Luminex assay (Fig. 6). There were no changes in the relative levels of cleaved PARP across the torpor-arousal cycle but active caspase-3 levels increased during EA and IA with respect to ET (to 2.15-fold and 2.4-fold of the EC level). The increase during EA was also significant with respect to EN.

Relative phosphorylation levels of STAT1-3 transcription factors

A Luminex assay was used to determine the relative levels of phosphorylation of p-STAT1 (Y701), p-STAT2 (Y690), and p-STAT3 (Y705) in thirteen-lined ground squirrel WAT over the six different time points (Fig. 7). There were no significant changes in the phosphorylation levels of p-STAT2 (Y690) over the torpor-arousal cycle. However, there was an approximate 2.25-fold increase in p-STAT1 (Y701) phosphorylation during LT compared to EC. Additionally, there was a significant decrease in p-STAT1 (Y701) phosphorylation during EA compared to LT, before increasing again during IA with respect to EA. Levels of p-STAT3 (Y705) also increased strongly by over 7-fold during LT with respect to EC but dropped again as animals aroused.

Relative protein and phosphorylation levels of upstream regulators to STATs

Immunoblotting was used to determine relative p-JAK phosphorylation levels as well as relative PIAS and SOCS protein levels in ground squirrel WAT. During EN, relative levels of p-JAK1 (Y1022/1023) significantly decreased to just below 25 % of the EC value and remained low in ET (Fig. 8). Phosphorylation levels then returned to approximately control values during LT, EA, and IA, values being 4.4–5.0 fold higher than values in EN. Phosphorylation levels of p-JAK2 (Y1007/1008) remained unchanged over the course of the torpor-arousal cycle. While there was no change in p-JAK3 (Y908) levels during EN, ET, and IA as compared with EC, p-JAK3 levels during ET, LT, and EA were significantly reduced to 60, 45, and 30 % of the EN value, respectively. This translated into a 53 and 35 % decrease in phosphorylation state of the proteins when comparing EC to LT and EA, respectively. Finally, p-JAK3 levels rose again during IA with respect to EA, returning to EC levels (Fig. 8). SOCS1 protein levels fell by about 50 % during EN and ET and then decreased further, reaching a low during LT at 30 % of the EC value which was significantly different from EC (Fig. 9). SOCS1 protein levels rose again

Fig. 3 Relative Bcl-xL protein and phosphorylation levels in ground squirrel WAT.

a Histogram showing mean standardized expression levels of Bcl-xL and p-Bcl-xL (S62) (\pm SEM, $n = 3$ –4 independent protein isolations from different animals, where $n = 3$ was used for p-Bcl-xL (S62) LT).

b Representative western blots. The top Bcl-xL band was quantified since it matched the expected molecular weight. Other information as in Fig. 2

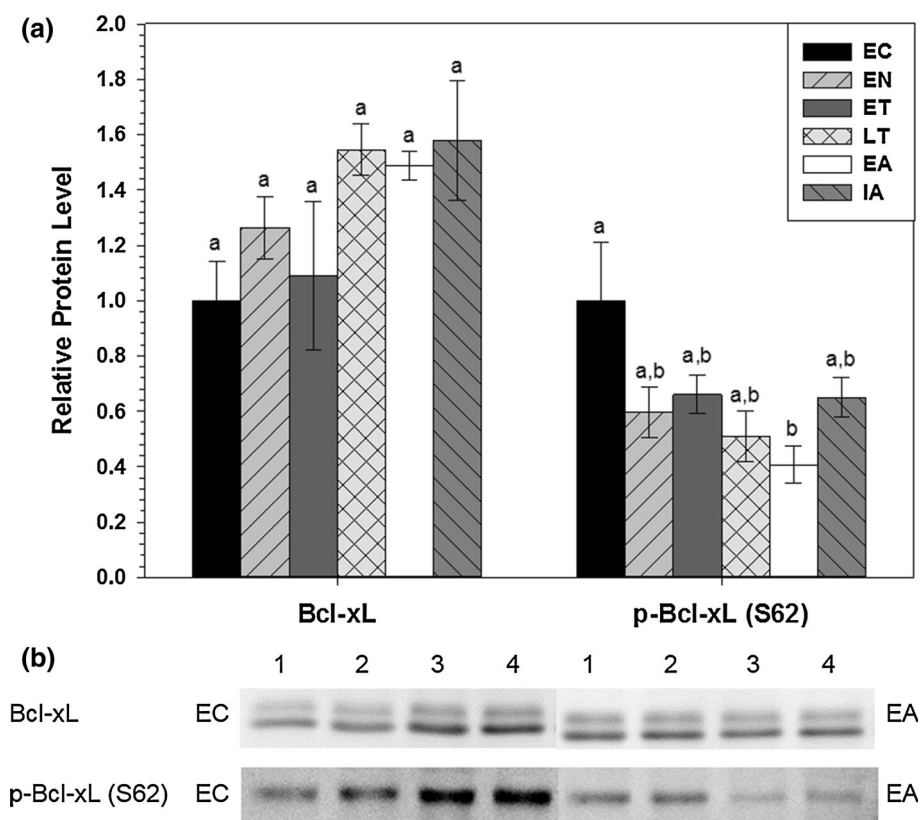


Fig. 4 Relative Mcl-1 protein and phosphorylation levels in ground squirrel WAT.

a Histogram showing mean standardized expression levels of Mcl-1 and p-Mcl-1 (S159) (\pm SEM, $n = 3$ –4 independent protein isolations from different animals, where $n = 3$ was used for p-Mcl-1 (S159) EC).

b Representative western blots. The top Mcl-1 band was quantified since it matched the expected molecular weight. Other information as in Fig. 2

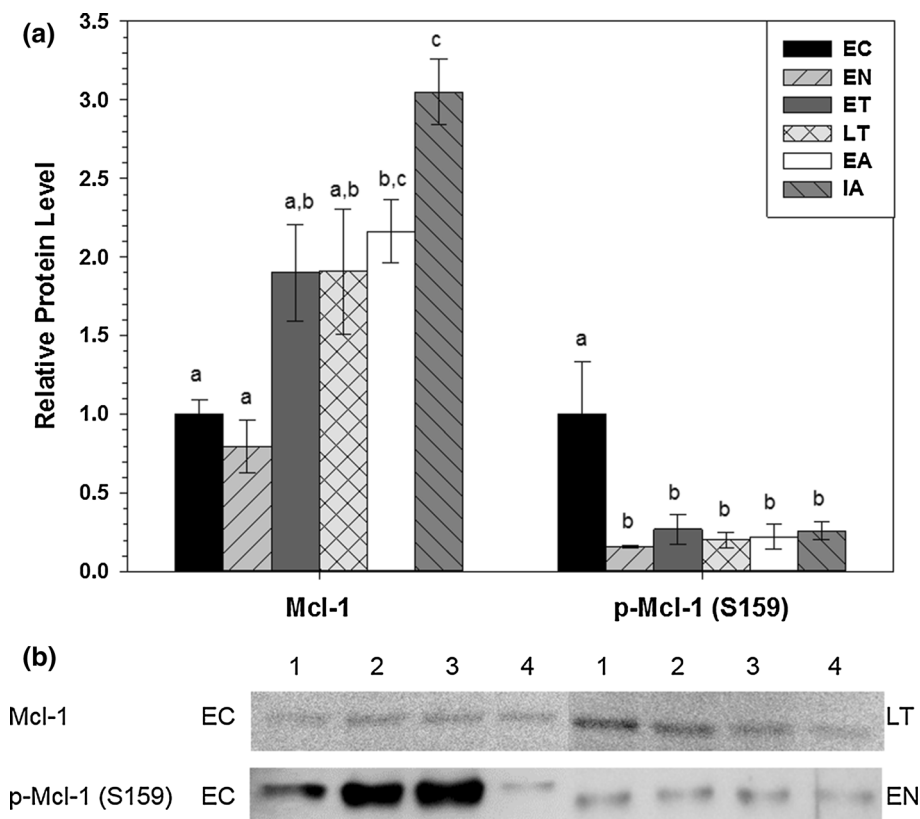


Fig. 5 Relative levels of x-IAP and c-IAP protein in ground squirrel WAT. **a** Histogram showing mean standardized expression levels of x-IAP and c-IAP (\pm SEM, $n = 4$ –8 independent protein isolations from different animals, where $n = 6$ was used for x-IAP EN and c-IAP ET, and $n = 8$ was used for c-IAP EN. **b** Representative western blots. Other information as in Fig. 2

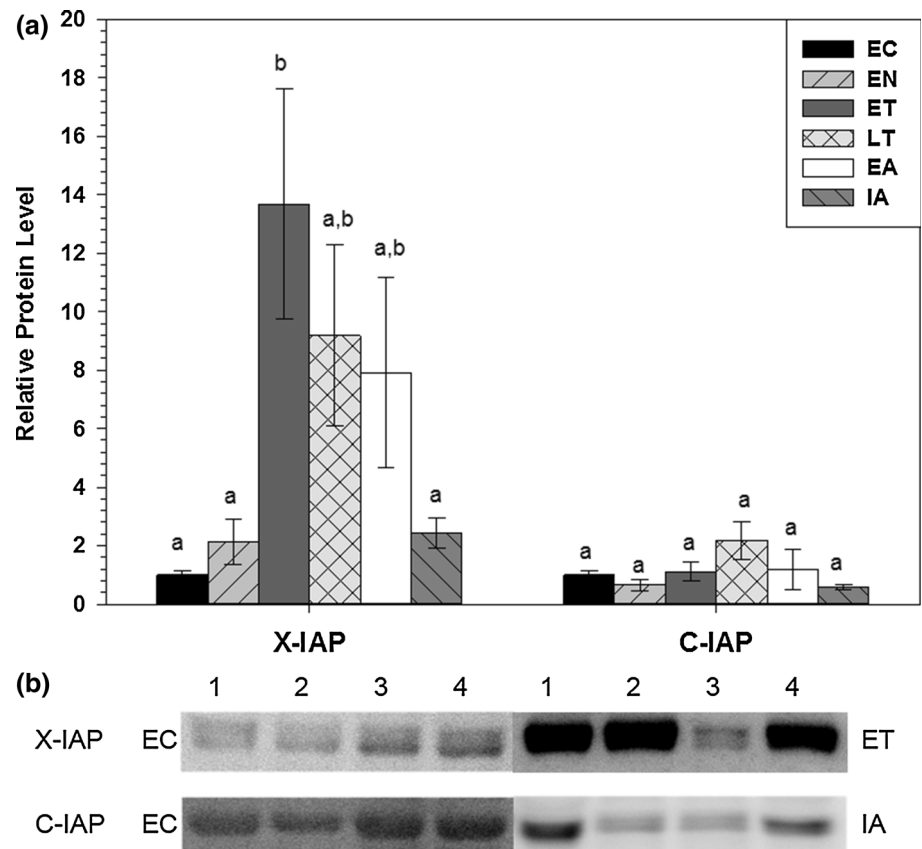
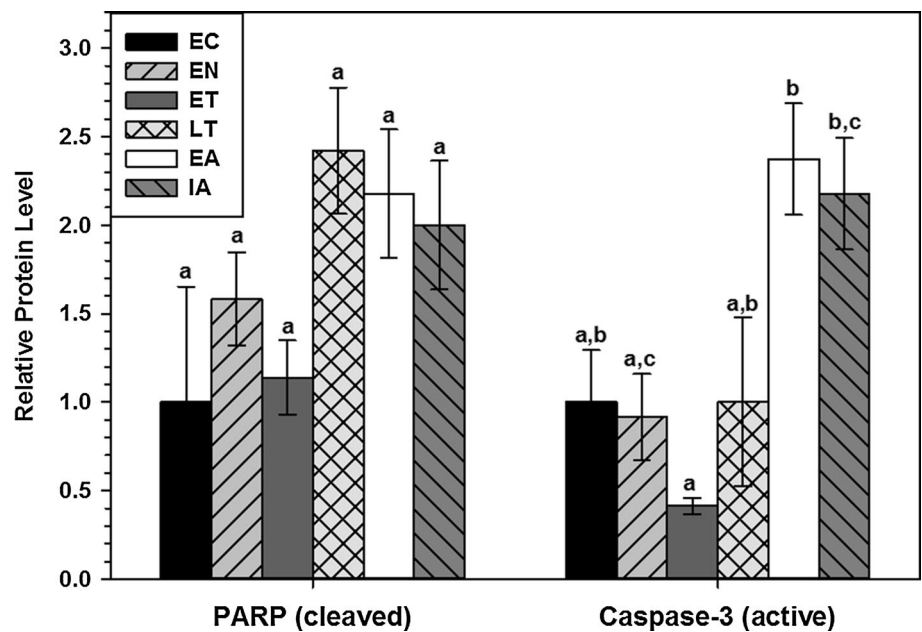


Fig. 6 Multiplex analysis of pro-apoptotic marker levels in ground squirrel WAT. Histogram showing mean relative expression levels of cleaved PARP and active caspase-3 (\pm SEM, $n = 3$ –4 independent protein isolations from different animals). Data were analyzed using ANOVA with a Tukey post hoc test. Shared letters indicate results that are not significantly different from each other and different letters indicate statistical significance ($p < 0.05$)



during EA and returned to control levels during IA. SOCS2 followed a similar pattern. Compared to the EC level, the level of SOCS2 protein decreased to 33, 41, 22, and 39 % of the EC value during EN, ET, LT, and EA, respectively.

However, SOCS2 levels rose again by 3.5-fold between LT and IA. SOCS3 protein levels dramatically decreased relative to EC during EN and remained low throughout the rest of the time course at levels that were just 8–28 % of the EC

Fig. 7 Multiplex analysis of STAT phosphorylation levels in ground squirrel WAT. Histogram showing mean relative expression levels of p-STAT1 (Y701), p-STAT2 (Y690), p-STAT3 (Y705) (\pm SEM, $n = 4$ independent protein isolations from different animals). Data were analyzed using ANOVA with a Tukey post hoc test. *Shared letters* indicate results that are not significantly different from each other and *different letters* indicate statistical significance ($p < 0.05$)

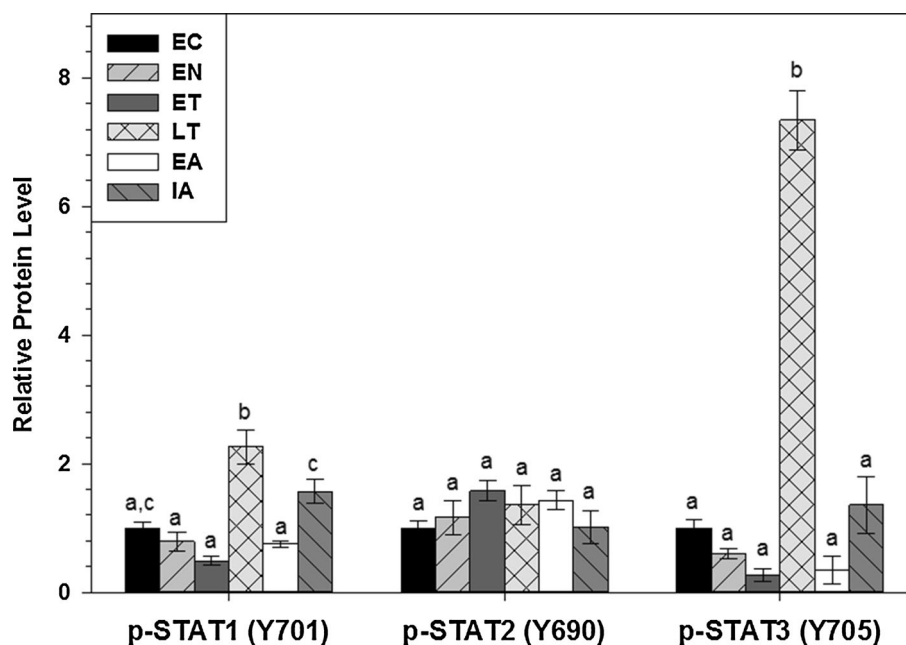
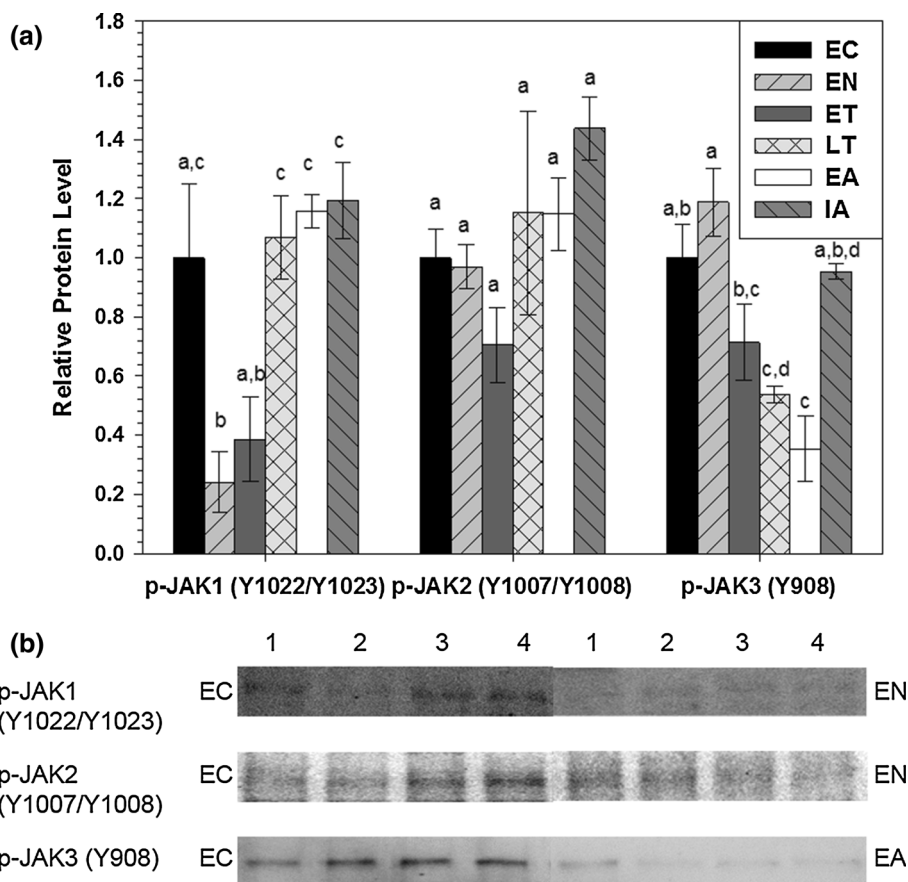


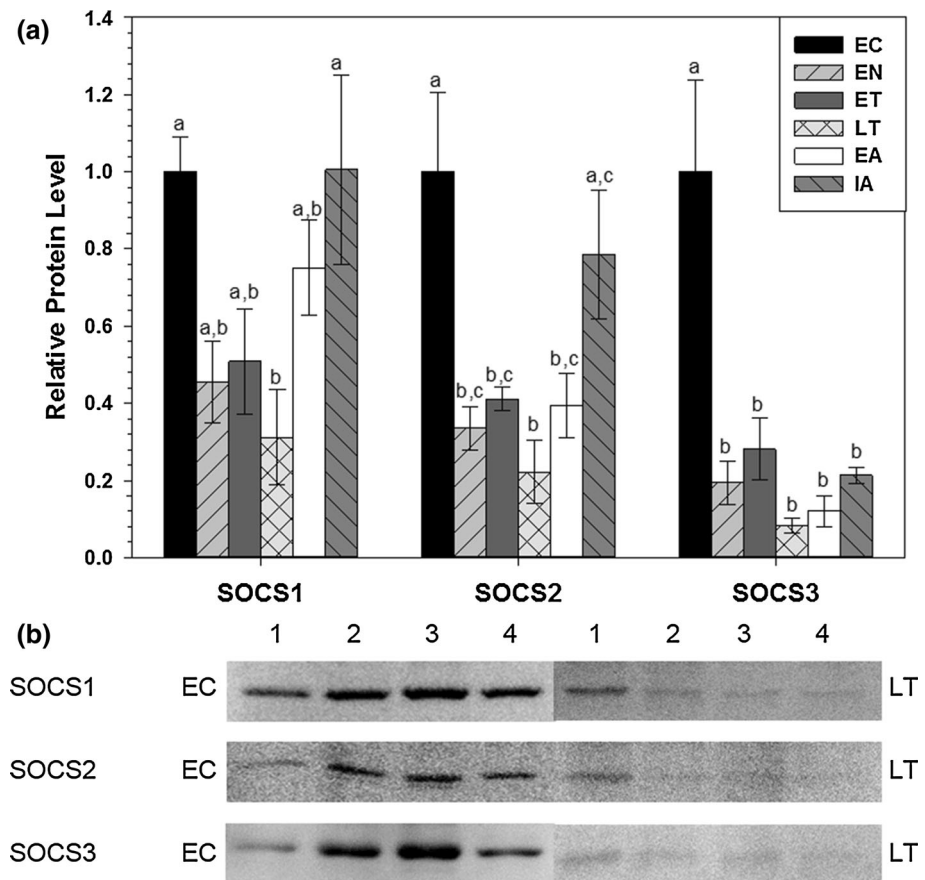
Fig. 8 Relative phosphorylation of JAK proteins in ground squirrel WAT. **a** Histogram showing mean standardized expression levels of p-JAK1 (Y1022/1023), p-JAK2 (Y1007/Y1008), and p-JAK3 (Y908) (\pm SEM, $n = 4$ independent protein isolations from different animals). **b** Representative western blots. Other information as in Fig. 2



value with levels being lowest in LT. There were no significant changes in relative PIAS1 protein levels over the torpor-arousal cycle (Fig. 10). However, PIAS3 levels

significantly increased by 1.9-fold in EA relative to EC levels but subsequently decreased dramatically during IA to just 20 % of the EA level (~40 % of the EC value).

Fig. 9 Relative levels of SOCS proteins in ground squirrel WAT. **a** Histogram showing mean standardized expression levels of SOCS1, SOCS2, and SOCS3 (\pm SEM, $n = 4$ independent protein isolations from different animals). **b** Representative western blots. Other information as in Fig. 2



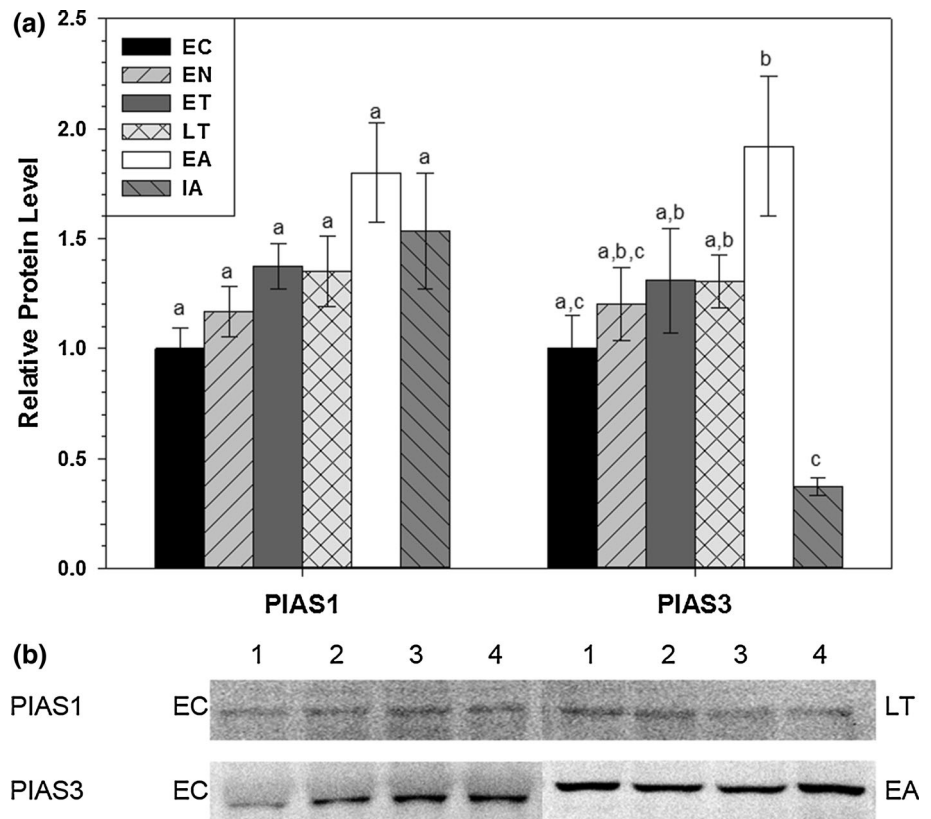
Discussion

In order to save energy and survive cold temperatures and lack of food during the winter months, many small mammals enter hibernation. The thirteen-lined ground squirrel (*Ictidomys tridecemlineatus*), like other hibernating mammals, survives these environmental conditions by suppressing all physiological functions and biochemical reactions to descend into torpor for long periods of time during which heart and breathing rates are strongly decreased [1, 4]. A strong suppression of metabolic rate, coupled with lowering of the hypothalamic set-point for body temperature, results in a decline in body temperature, often to as low as 0–5 °C during deep torpor [1, 4]. This entry into a hypometabolic state allows animals to maximize the time that they can survive until conditions are more favorable for active life, growth, and reproduction [33]. It is important to understand which genes are preferentially upregulated to preserve cell/tissue viability over the hibernating season. Previous studies have demonstrated that cytoprotective mechanisms are regulated in important organs such as the heart and brain over the torpor-arousal cycle [29, 31]. The reason to protect other tissues, like the white adipose tissue (WAT), might not be so apparent.

While hibernating, ground squirrels rely on fuel stores within their bodies for energy. As much as 60–80 % of the food consumed during the late summer period of hyperphagia is converted into fatty acids that are stored in WAT for subsequent consumption over the winter months [34]. Since β -fatty acids become the main metabolic fuel source during hibernation, and are required for the survival of all organs, it is imperative that metabolic adjustments be made to preserve the integrity of WAT and limit apoptosis that may otherwise be triggered by unfavorable environmental conditions [5]. Therefore, the focus of this study was to examine the role of anti-apoptotic proteins in ground squirrel WAT during hypometabolism. Despite the suppression of many energy-expensive processes during torpor, the present study suggests the upregulation or activation of selected anti-apoptotic proteins and related upstream regulators in ground squirrel WAT to support the torpor-arousal cycle.

The anti-apoptotic proteins Bcl-2, Mcl-1, and Bcl-xL play roles by preventing MOMP [13, 29, 35, 36]. Immunoblotting revealed differential protein expression and phosphorylation of these three proteins in WAT over the torpor-arousal cycle (Fig. 2, 3, 4). The results showed that the total Bcl-2 protein levels decreased to

Fig. 10 Relative levels of PIAS1 and PIAS3 protein in ground squirrel WAT. **a** Histogram showing mean standardized expression levels of PIAS1 and PIAS3 (\pm SEM, $n = 4$ independent protein isolations from different animals). **b** Representative western blots. Other information as in Fig. 2



approximately 13–45 % of the EC value between ET and IA. Bcl-2 phosphorylation at serine-70 is known to increase the anti-apoptotic function of Bcl-2 [37]. However, the significant decrease in the relative phosphorylation levels of p-Bcl-2 (S70) seen during LT suggests that the anti-apoptotic action of Bcl-2, as mediated via effectors that alter S70 phosphorylation, is not employed during torpor. Bcl-2 phosphorylation at threonine 56 has the opposite effect on the protein—it is known to suppress Bcl-2 anti-apoptotic activity [38]. Therefore, by contrast with the results for p-Bcl-2 (S70) phosphorylation, the relative decrease in p-Bcl-2 (T56) throughout torpor and arousal (compared to EC) suggests an activation of Bcl-2 mediated via the T56 site. Together, the opposite effects that reduced serine and threonine-phosphorylated forms of Bcl-2 create, underscores the regulatory complexity of anti-apoptotic pathways, but ultimately suggests that the changes may cancel each other out. Together with the reduced total protein levels, this suggests a minor role for Bcl-2 in the regulation of apoptosis in WAT over the torpor-arousal cycle. Unlike Bcl-2, the data suggest that Mcl-1 plays an anti-apoptotic role in WAT during hibernation, particularly during arousal. Mcl-1 total protein showed a rising trend during torpor and was significantly increased by 2–3 fold during EA and IA. Arousing ground squirrels experience a rapid rise in T_b due to shivering and nonshivering

thermogenesis that is fueled by a very rapid increase in oxygen uptake and consumption, which also triggers increased reactive oxygen species (ROS) generation [1, 2]. As a result, strong antioxidant defenses are needed during hibernation and enhanced anti-apoptosis mechanisms would complement this by helping to defend against apoptosis triggered by oxidative stress. Furthermore, it has been demonstrated in mice cell lines that Mcl-1 has a short half-life ranging between 30 min to 3 h [40]. Since ground squirrels can enter periods of hypometabolism that can be many days long [1], the present data suggest that Mcl-1 may have to be continuously translated during hibernation or stabilized by post-translational modifications. Since energy-expensive processes would need to be promoted to elevate Mcl-1 protein levels during hibernation, this can indicate that Mcl-1 plays an essential function in WAT anti-apoptosis. Phosphorylation of Mcl-1 at serine 159 (S159) by kinases such as glycogen synthase kinase 3 β (GSK3 β) recruits ubiquitinases, like the E3 ligase Mule, which target Mcl-1 for degradation [41, 42]. However, immunoblotting demonstrated that the relative levels of phosphorylated forms of Mcl-1 (S159) were suppressed throughout the torpor-arousal cycle (compared to EC) despite an increase in total Mcl-1 protein (Fig. 4). Therefore, this implies that proteolysis of WAT Mcl-1 may be strongly suppressed throughout the torpor-arousal cycle

and suggests that Mcl-1 may play a more substantial role in cytoprotection than Bcl-2. Lastly, Bcl-xL protein levels in WAT did not change throughout the hibernation bout. In a similar study, total protein levels of Bcl-xL were also shown to be stable during LT relative to EC in brown adipose tissue (BAT), skeletal muscle, and liver of thirteen-lined ground squirrels, although they decreased during LT in cardiac muscle and kidney, and increased in brain [41]. Furthermore, relative phosphorylation of Bcl-xL (S62) in WAT showed a general pattern of reduced levels that was significant during EA (relative to EC) (Fig. 3). Bcl-xL phosphorylation at serine 62 is known to decrease Bcl-xL affinity for Bax, which leads to Bax oligomerization and MOMP [42, 43]. Although Bcl-xL protein levels remain constant over the torpor-arousal cycle, the reduction in S62 phosphorylation could activate Bcl-xL to contribute to cell survival efforts during the arousal period, when ROS can initiate apoptotic signaling events. The present results suggest that Mcl-1, and perhaps Bcl-xL, play an active anti-apoptotic role in WAT of hibernating ground squirrels.

Members of the inhibitor of apoptosis protein (IAP) family provide a non-mitochondrial mechanism to promote cell survival. They have known functions in regulating caspase activity, cell proliferation, cell survival pathways, and many other important cellular events [14]. Caspases are cysteine proteases that are crucial players in the destructive events of apoptosis [14]. They are known to be activated and attack normal cells in times of nutrient deprivation, hypoxia, and DNA damage—all conditions that could occur during mammalian hibernation, as a consequence of harsh environmental conditions [14]. Thus, it was deemed essential to study x-IAP and c-IAP1/2 using immunoblotting techniques to determine their role in thirteen-lined ground squirrel WAT cell survival. Levels of c-IAP1/2 did not change over the course of the torpor-arousal cycle but x-IAP levels increased strongly during ET and remained elevated throughout LT and EA (Fig. 5). These data suggest that x-IAP may serve as an important anti-apoptotic protein during torpor when cells may be coping with cellular stress brought on by low body temperatures, low oxygen levels, respiratory acidosis (due to apnoic breathing patterns), and low cellular energy (ATP) availability [3, 4]. The literature states that x-IAP directly binds caspase-3, caspase-7, and caspase-9, whereas c-IAP1 and c-IAP2 inhibit TNF- α activation of caspase-8 [14, 15]. These three IAP proteins function as E3 ligases that target caspases for polyubiquitylation, which has been linked to caspase inhibition through degradative and non-degradative pathways [14]. In the case of the thirteen-lined ground squirrels, x-IAP is significantly upregulated in WAT to inhibit caspases-3, -7, and -9 which are activated by the intrinsic apoptotic pathway. Therefore, hibernating ground squirrel upregulation of x-IAP in WAT serves as a possible

non-mitochondrial mechanism of inhibiting apoptosis and prolonging cell survival. Although it can be argued that c-IAP protein levels are not upregulated during the torpor-arousal cycle, the extrinsic apoptotic pathway can be inhibited by x-IAP because caspase-8 must activate caspase-3 to initiate apoptosis and x-IAP is a known inhibitor of caspase-3 [12]. While both x-IAP and c-IAP1/2 suppress apoptosis by acting on caspases, the present results demonstrate that x-IAP expression is stress responsive, further indicating that select anti-apoptotic proteins are promoting cell survival throughout the torpor-arousal cycle in ground squirrel WAT.

To confirm that WAT cells were indeed protected from undergoing apoptosis, relative cleaved PARP, and active caspase-3 levels were analyzed across the torpor-arousal cycle (Fig. 6). Cleaved PARP inhibits the DNA repair activity of uncleaved PARP, while caspase-3 is a protease, and both proteins serve as markers of cell death [39]. Cleaved PARP levels remained constant across the torpor-arousal cycle, while active caspase-3 levels increased during EA and IA, relative to EN, but not significantly different with respect to euthermic levels. Together, these data suggest that apoptosis events are generally subdued during torpor but may be more prevalent during the arousal phase, possibly to initiate the controlled destruction of cells damaged during the torpor-arousal cycle by cold stress, DNA damage caused by ROS, or ischemia–reperfusion injury. Additionally, these results help confirm that anti-apoptotic proteins such as Mcl-1, Bcl-xL, and x-IAP have important, cytoprotective roles during torpor.

A Luminex assay was used to assess the relative levels of phosphorylated forms of p-STAT1 (Y701), p-STAT2 (Y690), and p-STAT3 (Y705) in thirteen-lined ground squirrel WAT over the torpor-arousal cycle. Phosphorylated STAT1 can upregulate genes that code for proteins that lead to cell death, including Bax and Bak1, and this has established STAT1 as a protein target for tumor suppression [43, 44]. Ground squirrel WAT showed an increase in p-STAT1 (Y701) levels during LT, followed by a subsequent decrease in EA and then a modest rise again in IA (Fig. 7). Elevated phosphorylated STAT1 during LT could correlate with potentially harmful cellular conditions accompanying torpor, causing WAT cells to express stress-responsive genes and proteins involved in cell death. STAT1 is a known inducer of apoptosis in many tissues in response to ischemia/reperfusion. Ischemia could be experienced during torpor when blood becomes thicker at low temperature, and breathing rates slow down, resulting in a diminished supply of oxygen to hibernator tissues [3, 18, 24, 45]. In contrast, reperfusion (a restoration of normal blood flow to the tissues) occurs as the hibernator warms up and breathing/heart rates increase again. This physiological change would be best represented during EA.

Phosphorylated STAT1 (Y701) levels increased most strongly during LT and IA. This suggests that STAT1 is activated in response to apoptotic stimuli associated with low core body temperature and oxygen availability during LT and the aftermath of rapidly increasing body temperature upon arousal and the presence of ROS during IA. Expression of p-STAT2 did not change over the course of the torpor-arousal cycle which is not surprising since STAT2 is known to be associated with the immune response and not with apoptosis control [23, 44]. However, p-STAT3 levels did increase very strongly during LT and STAT3 is known to regulate the expression of genes that increase cell survival, including Mcl-1, Bcl-2, Bcl-xL, Survivin, and x-IAP, which makes it a popular target for cancer therapeutics [35, 44]. Phosphorylated STAT3 levels increased over 7-fold during LT, and then decreased again during EA and IA (Fig. 7). These data suggest that the transcription of genes involved in anti-apoptosis is important during late torpor, when significant cell damage may have accumulated or in anticipation of apoptosis-inducing signals that could occur during the arousal process. The present results suggest that increased levels of Mcl-1 during EA and IA correspond with the increase of p-STAT3 during LT, given that changes in post-translational modifications may also be at play by prolonging the half-life of proteins. Protein expression of Mcl-1, Bcl-2, and Bcl-xL suggest that LT-induced phosphorylation of STAT1 and STAT3 may be responsible for the elevation of Mcl-1 protein specifically in WAT of hibernating ground squirrels (Fig. 2, 3, 4, 7).

Protein inhibitors of activated STATs (PIAS) are able to inhibit STATs and other TFs by blocking their DNA-binding ability, functioning as SUMO E3 ligases, and recruiting co-repressors like histone deacetylases [20, 26, 46]. PIAS1 blocks STAT1 activity by preventing DNA-binding activity [26, 28, 47]. However, PIAS1 expression did not change over the course of the torpor-arousal cycle and this suggests that PIAS inhibition of STAT1 is not required to limit pro-apoptotic gene expression. Instead, other mechanisms of apoptosis inhibition may dominate, such as STAT3-mediated expression of anti-apoptotic proteins like Bcl-2, Bcl-xL, and Mcl-1. PIAS3 expression increased during EA and then decreased during IA to 20 % of the EA level (Fig. 10). PIAS3 inhibits p-STAT3, which increased 7.3-fold in ground squirrel WAT during LT (Fig. 7) [19, 28, 47]. The increase in PIAS3 expression during EA could be a result of the rapid increase in p-STAT3 levels during LT, in order to coordinate the timely expression of STAT-inducible genes.

Levels of p-JAK1 (Y1022/Y1023) decreased significantly during EN, remained low in EA, and then returned to EC levels during LT, EA, and IA. Phosphorylated JAK3 (Y908) levels decreased in LT and EA but by contrast,

p-JAK2 (Y1007/1008) levels did not change (Fig. 8). It was hypothesized that phosphorylation of JAK1-3 (which activates these kinases) would increase to promote STAT activation and the expression of anti-apoptotic genes in WAT cells. Instead, p-JAK1 and p-JAK3 levels decreased which could be due to several factors including reduced cytokine or growth hormone signaling, or increases in the expression of JAK1 inhibitors such as SOCS1 and SOCS3 [19, 48]. From a conservation of energy standpoint, it would be favorable to decrease JAK1 and JAK3 phosphorylation levels during hibernation because these kinases can upregulate all seven STATs, but not all of the STAT target genes are required during torpor. Certain STAT target gene products are required only at specific time points during hibernation. Since there were no changes in p-JAK1-3 levels that could increase the phosphorylation of STATs 1-3, it seems that a different mechanism of STAT activation is required in the WAT cells of hibernating thirteen-lined ground squirrels. JAKs are the dominant activators of STATs but other protein kinases can also phosphorylate STATs. For example, STAT3 can be phosphorylated by non-receptor tyrosine kinases like Src and Abelson (Abl) or by transmembrane G-protein-coupled receptors like serotonin 5-HT_{2A} receptor and angiotensin II receptor [16, 17, 25]. Furthermore, the EGFR signaling pathway has been implicated in STAT phosphorylation and subsequent signaling in prostate cancer and head and neck squamous carcinoma cells [16, 25]. Hence, further studies are required to better understand the mechanisms of STAT regulation in WAT during hibernation.

As expected, SOCS protein expression changed over the course of the torpor-arousal cycle, levels of the three proteins being reduced uniformly during entrance and during early and late torpor but each protein responded differently during arousal. In particular, SOCS1 expression decreased to approximately 30 % of the euthermic value during LT before returning to EC levels during EA/IA whereas SOCS3 expression remained below 30 % of the EC value over the full course of the torpor-arousal cycle. SOCS2 expression was found to decrease to 40 % of EC between EN and EA, before it rose again to EC levels during IA (Fig. 9). SOCS1 and SOCS3 can inhibit JAKs by targeting JAKs and JAK receptors for ubiquitination and degradation, by binding JAKs to inhibit STAT phosphorylation, and by the direct inhibition of JAK activity [19, 27, 28, 47]. SOCS2 can inhibit SOCS family members such as SOCS1 and can selectively inhibit JAK2–STAT3 signaling in some cancer cells [27, 48, 49]. Interestingly, a downregulation in SOCS expression should be accompanied by an upregulation of JAK phosphorylation but in general, p-JAK levels remained constant or decreased in hibernating thirteen-lined ground squirrel WAT. It is possible that post-translational modifications like methylation, acetylation, and

ubiquitination could be more influential sources of JAK inhibition during hibernation than SOCS activity. Additionally, SOCS are feedback-loop inhibitors since STATs are able to bind to SOCS promoters and initiate their transcription [26, 49, 50]. The low relative abundance of SOCS1–3 throughout the torpor-arousal cycle suggests highly controlled STAT-induced expression of specific target genes, further suggesting that the genes that are upregulated by STATs (including members of the anti-apoptotic Bcl-2 family) have important roles to play in WAT of hibernating ground squirrels.

It has been calculated that hibernation saves ground squirrels about 90 % of the energy that would otherwise be needed to sustain euthermia throughout the winter [1]. These huge energy savings are necessary for survival but come with challenges because hibernator cells can be subject to stressful conditions, including hypoxia, ischemia, cold temperatures, and elevated ROS, etc. over the course of torpor-arousal. All cells need added cytoprotection during this time. Ensuring the survival of WAT cells is necessary to ensure the survival of the hibernator, since the triglycerides stored in WAT are the main source of fuel for nearly all tissues/organs during the hibernating months. The present study analyzed the relative abundance of total/phosphorylated anti-apoptotic Bcl-2 family proteins, IAPs, and their upstream regulators (p-STATs, p-JAKs, SOCS, and PIAS), as well as cell death markers PARP (cleaved) and caspase-3 (active) over the course of the torpor-arousal cycle. Significant increases in Mcl-1 and x-IAP during the hibernation bout suggested that these proteins serve as important inhibitors of apoptosis in WAT of hibernating ground squirrels, with Bcl-2 and Bcl-xL playing a lesser role. Unchanging levels of cleaved PARP and active caspase-3 with respect to EC indicate that pro-survival protein activity likely outweighs the negative effects of pro-apoptotic proteins. Unique changes in protein expression and phosphorylation levels were found for the upstream regulators of pro- and anti-apoptotic signaling. Major increases in p-STAT1 and p-STAT3 levels during LT suggest that hibernation-induced pro-apoptotic signals lead to the transcription of both cell death and survival proteins, which control apoptosis at both the mitochondrial level and downstream of the mitochondria. STAT1 is known to regulate cell differentiation and energy catabolism in addition to apoptosis, so increases in p-STAT1 levels could also suggest the inhibition of energy-expensive processes like adipocyte proliferation and differentiation [44, 51]. Decreases in corresponding p-JAKs suggest that non-JAK–STAT pathway kinases like Src or Abl may control the activation of STATs during hibernation. The lack of change in PIAS1 levels could indicate that STAT-3-mediated expression of anti-apoptotic proteins is sufficient to inhibit cell death induced by STAT1 gene expression.

Additionally, increases in PIAS3 during EN could be important to limit STAT3-mediated gene expression to certain time points during hibernation. Finally, reduced SOCS1–3 levels suggest low levels of feedback inhibition of the JAK–STAT pathway, possibly due to selective expression of certain genes like Mcl-1 and x-IAP. The present study suggests a putative role for anti-apoptotic pathways in WAT during the torpor-arousal cycle. These results can be complemented with additional studies that use larger sample sizes to assess other pro-apoptotic targets such as Bax, Bim, Bad, etc., to assay which relative amounts of genomic DNA cleavage, and to measure caspase cleavage products, which may further support that there are few apoptotic events in WAT over the torpor-arousal cycle of ground squirrel hibernation.

Acknowledgments Thanks to J.M. Storey for editorial review of this manuscript. This work was supported by a Discovery Grant (#6793) from the Natural Sciences and Engineering Research Council of Canada. KBS holds the Canada Research Chair in Molecular Physiology, BEL holds an NSERC Canada Graduate Scholarship, and SML held an NSERC Undergraduate Summer Research Award.

References

1. Storey KB, Heldmaier G, Rider MH (2010) Mammalian hibernation: Physiology, cell signaling, and gene control on metabolic rate depression. In: Lubzens E (ed) *Dormancy and resistance in harsh environments*. Springer-Verlag, Berlin, Heidelberg, pp 227–252
2. Storey KB (2010) Out cold: biochemical regulation of mammalian hibernation—a mini-review. *Gerontology* 56:220–230. doi:[10.1159/000228829](https://doi.org/10.1159/000228829)
3. Storey KB, Storey JM (2004) Mammalian hibernation: biochemical adaptation and gene expression. In: Storey KB (ed) *Functional metabolism: regulation and adaptation*. Wiley Inc., Hoboken, pp 443–472
4. Wang LCH, Lee TF (1996) Torpor and hibernation in mammals: metabolic, physiological, and biochemical adaptations. In: *Handbook of physiology—environmental physiology*, pp 507–532
5. Sheriff MJ, Fridinger RW, Tøien Ø, Barnes BM, Buck CL (2013) Metabolic rate and prehibernation fattening in free-living arctic ground squirrels. *Physiol Biochem Zool* 86:515–527. doi:[10.1086/673092](https://doi.org/10.1086/673092)
6. Alkhouri N, Gornicka A, Berk MP, Thapaliya S, Dixon LJ, Kashyap S, Schauer PR, Feldstein AE (2010) Adipocyte apoptosis, a link between obesity, insulin resistance, and hepatic steatosis. *J Biol Chem* 285:3428–3438. doi:[10.1074/jbc.M109.074252](https://doi.org/10.1074/jbc.M109.074252)
7. Gullicksen PS, Hausman DB, Dean RG, Hartzell DL, Baile CA (2003) Adipose tissue cellularity and apoptosis after intracerebroventricular injections of leptin and 21 days of recovery in rats. *Int J Obes Relat Metab Disord* 27:302–312. doi:[10.1038/sj.ijo.0802205](https://doi.org/10.1038/sj.ijo.0802205)
8. Herold C, Rennekampff HO, Engeli S (2013) Apoptotic pathways in adipose tissue. *Apoptosis* 18:911–916. doi:[10.1007/s10495-013-0848-0](https://doi.org/10.1007/s10495-013-0848-0)
9. Taylor RC, Cullen SP, Martin SJ (2008) Apoptosis: controlled demolition at the cellular level. *Nat Rev Mol Cell Biol* 9:231–241. doi:[10.1038/nrm2312](https://doi.org/10.1038/nrm2312)

10. Spierings D, McStay G, Saleh M, Bender C, Chipuk J, Maurer U, Green DR (2005) Connected to death: the (unexpurgated) mitochondrial pathway of apoptosis. *Science* 310:66–67. doi:[10.1126/science.1117105](https://doi.org/10.1126/science.1117105)
11. Labi V, Erlacher M (2015) How cell death shapes cancer. *Cell death* 6:e1675. doi:[10.1038/cddis.2015.20](https://doi.org/10.1038/cddis.2015.20)
12. Tinahones FJ, Coín Aragüez L, Murri M, Oliva Olivera W, Mayas Torres MD, Barbarroja N, Gomez Huelgas R, Malagón MM, El Bekay R (2013) Caspase induction and BCL2 inhibition in human adipose tissue: a potential relationship with insulin signaling alteration. *Diabetes Care* 36:513–521. doi:[10.2337/dc12-0194](https://doi.org/10.2337/dc12-0194)
13. Chipuk JE, Moldoveanu T, Llambi F, Parsons MJ, Green DR (2010) The BCL-2 family reunion. *Mol Cell* 37:299–310. doi:[10.1016/j.molcel.2010.01.025](https://doi.org/10.1016/j.molcel.2010.01.025)
14. Gyrd-Hansen M, Meier P (2010) IAPs: from caspase inhibitors to modulators of NF-kappaB, inflammation and cancer. *Nat Rev Cancer* 10:561–574. doi:[10.1038/nrc2979](https://doi.org/10.1038/nrc2979)
15. Perez HL, Chaudhry C, Emanuel SL, Fanslau C, Fargnoli J, Gan J, Kim KS, Lei M, Naglich JG, Traeger SC, Vuppugalla R, Wei DD, Vite GD, Talbott RL, Borzilleri RM (2015) Discovery of potent heterodimeric antagonists of inhibitor of apoptosis proteins (IAPs) with sustained antitumor activity. *J Med Chem* 58:1556–1562. doi:[10.1021/jm501482t](https://doi.org/10.1021/jm501482t)
16. Al Zaid Siddiquee K, Turkson J (2008) STAT3 as a target for inducing apoptosis in solid and hematological tumors. *Cell Res* 18:254–267. doi:[10.1038/cr.2008.18](https://doi.org/10.1038/cr.2008.18)
17. Subramaniam A, Shanmugam MK, Perumal E, Li F, Nachiyappan A, Dai X, Swamy SN, Ahn KS, Kumar AP, Tan BKH, Hui KM, Sethi G (2013) Potential role of signal transducer and activator of transcription (STAT)3 signaling pathway in inflammation, survival, proliferation and invasion of hepatocellular carcinoma. *Biochim Biophys Acta: Rev Cancer* 1835:46–60. doi:[10.1016/j.bbcan.2012.10.002](https://doi.org/10.1016/j.bbcan.2012.10.002)
18. Stephanou A, Latchman DS (2003) STAT-1: a novel regulator of apoptosis. *Int J Exp Pathol* 84:239–244. doi:[10.1111/j.0959-9673.2003.00363.x](https://doi.org/10.1111/j.0959-9673.2003.00363.x)
19. Kiu H, Nicholson SE (2012) Biology and significance of the JAK/STAT signalling pathways. *Growth Factors* 30:88–106. doi:[10.3109/08977194.2012.660936](https://doi.org/10.3109/08977194.2012.660936)
20. Shuai K, Liu B (2005) Regulation of gene-activation pathways by PIAS proteins in the immune system. *Nat Rev Immunol* 5:593–605. doi:[10.1038/nri1667](https://doi.org/10.1038/nri1667)
21. Alvarez JV, Frank DA (2004) Genome-wide analysis of STAT target genes: elucidating the mechanism of STAT-mediated oncogenesis. *Cancer Biol Ther* 3:1045–1050. doi:[10.4161/cbt.3.11.1172](https://doi.org/10.4161/cbt.3.11.1172)
22. Koch V, Staab J, Ruppert V, Meyer T (2012) Two glutamic acid residues in the DNA-binding domain are engaged in the release of STAT1 dimers from DNA. *BMC Cell Biol* 13:22. doi:[10.1186/1471-2121-13-22](https://doi.org/10.1186/1471-2121-13-22)
23. Siveen KS, Sikka S, Surana R, Dai X, Zhang J, Kumar AP, Tan BKH, Sethi G, Bishayee A (2014) Targeting the STAT3 signaling pathway in cancer: role of synthetic and natural inhibitors. *Biochim Biophys Acta* 1845:136–154. doi:[10.1016/j.bbcan.2013.12.005](https://doi.org/10.1016/j.bbcan.2013.12.005)
24. Kumar A, Commene M, Flickinger TW, Horvath CM, Stark GR (1997) Defective TNF-alpha-induced apoptosis in STAT1-null cells due to low constitutive levels of caspases. *Science* 278:1630–1632. doi:[10.1126/science.278.5343.1630](https://doi.org/10.1126/science.278.5343.1630)
25. Yu H, Jove R (2004) The STATs of cancer—new molecular targets come of age. *Nat Rev Cancer* 4:97–105. doi:[10.1038/nrc1275](https://doi.org/10.1038/nrc1275)
26. Furqan M, Mukhi N, Lee B, Liu D (2013) Dysregulation of JAK-STAT pathway in hematological malignancies and JAK inhibitors for clinical application. *Biomark Res* 1:1–5. doi:[10.1186/2050-7771-1-5](https://doi.org/10.1186/2050-7771-1-5)
27. Tamiya T, Kashiwagi I, Takahashi R, Yasukawa H, Yoshimura A (2011) Suppressors of cytokine signaling (SOCS) proteins and JAK/STAT pathways: regulation of T-cell inflammation by SOCS1 and SOCS3. *Arterioscler Thromb Vasc Biol* 31:980–985. doi:[10.1161/ATVBAHA.110.207464](https://doi.org/10.1161/ATVBAHA.110.207464)
28. Valentino L, Pierre J (2006) JAK/STAT signal transduction: regulators and implication in hematological malignancies. *Biochem Pharmacol* 71:713–721. doi:[10.1016/j.bcp.2005.12.017](https://doi.org/10.1016/j.bcp.2005.12.017)
29. Rouble AN, Hefler J, Mamady H, Storey KB, Tessier SN (2013) Anti-apoptotic signaling as a cytoprotective mechanism in mammalian hibernation. *Peer J* 1:e29. doi:[10.7717/peerj.29](https://doi.org/10.7717/peerj.29)
30. McMullen DC, Hallenbeck JM (2010) Regulation of Akt during torpor in the hibernating ground squirrel, *Ictidomys tridecemlineatus*. *J Comp Physiol B Biochem Syst Environ Physiol* 180:927–934. doi:[10.1007/s00360-010-0468-8](https://doi.org/10.1007/s00360-010-0468-8)
31. Luu BE, Tessier SN, Duford DL, Storey KB (2015) The regulation of troponins I, C and ANP by GATA4 and Nk2–5 in heart of hibernating thirteen-lined ground squirrels. *PLoS ONE* 10:e0117747. doi:[10.1371/journal.pone.0117747](https://doi.org/10.1371/journal.pone.0117747)
32. Rouble AN, Tessier SN, Storey KB (2014) Characterization of adipocyte stress response pathways during hibernation in thirteen-lined ground squirrels. *Mol Cell Biochem* 393:271–282. doi:[10.1007/s11010-014-2070-y](https://doi.org/10.1007/s11010-014-2070-y)
33. Storey KB (2015) Regulation of hypometabolism: insights into epigenetic controls. *J Exp Biol* 218:150–159. doi:[10.1242/jeb.106369](https://doi.org/10.1242/jeb.106369)
34. Boyer BB, Barnes BM (1999) Molecular and metabolic aspects of mammalian hibernation. *Bioscience* 49:713–724. doi:[10.2307/1313595](https://doi.org/10.2307/1313595)
35. Carpenter RL, Lo HW (2014) STAT3 target genes relevant to human cancers. *Cancers* 6:897–925. doi:[10.3390/cancers6020897](https://doi.org/10.3390/cancers6020897)
36. Bah N, Maillet L, Ryan J, Dubreil S, Gautier F, Letai A, Juin P, Barillé-Nion S (2014) Bcl-xL controls a switch between cell death modes during mitotic arrest. *Cell Death Dis* 5:e1291. doi:[10.1038/cddis.2014.251](https://doi.org/10.1038/cddis.2014.251)
37. Blagosklonny MV (2001) Unwinding the loop of Bcl-2 phosphorylation. *Leuk Off J Leuk Soc Am Leuk Res Fund UK* 15:869–874. doi:[10.1038/sj.leu.2402134](https://doi.org/10.1038/sj.leu.2402134)
38. De Chiara G, Marcocci ME, Torcia M, Lucibello M, Rosini P, Bonini P, Higashimoto Y, Damonte G, Armirotti A, Amodei S, Palamara AT, Russo T, Garaci E, Cozzolino F (2006) Bcl-2 phosphorylation by p38 MAPK: identification of target sites and biologic consequences. *J Biol Chem* 281:21353–21361. doi:[10.1074/jbc.M511052200](https://doi.org/10.1074/jbc.M511052200)
39. D'Amours D, Sallmann FR, Dixit VM, Poirier GG (2001) Gain-of-function of poly(ADP-ribose) polymerase-1 upon cleavage by apoptotic proteases: implications for apoptosis. *J Cell Sci* 114:3771–3778
40. Zhao J, Xin M, Wang T, Zhang Y, Deng X (2009) Nicotine enhances the antiapoptotic function of Mcl-1 through phosphorylation. *Mol Cancer Res* 7:1954–1961. doi:[10.1158/1541-7786.MCR-09-0304](https://doi.org/10.1158/1541-7786.MCR-09-0304)
41. Ren H, Koo J, Guan B, Yue P, Deng X, Chen M, Khuri FR, Sun S-Y (2013) The E3 ubiquitin ligases β -TrCP and FBXW7 cooperatively mediates GSK3-dependent Mcl-1 degradation induced by the Akt inhibitor API-1, resulting in apoptosis. *Mol Cancer* 12:146. doi:[10.1186/1476-4598-12-146](https://doi.org/10.1186/1476-4598-12-146)
42. Maurer U, Charvet C, Wagman AS, Dejardin E, Green DR (2006) Glycogen synthase kinase-3 regulates mitochondrial outer membrane permeabilization and apoptosis by destabilization of MCL-1. *Mol Cell* 21:749–760. doi:[10.1016/j.molcel.2006.02.009](https://doi.org/10.1016/j.molcel.2006.02.009)
43. Satoh JI, Tabunoki H (2013) A comprehensive profile of ChIP-Seq-based STAT1 target genes suggests the complexity of

- STAT1-mediated gene regulatory mechanisms. *Gene Regul Syst Bio* 2013:41–56. doi:[10.4137/GRSB.S11433](https://doi.org/10.4137/GRSB.S11433)
44. Calò V, Migliavacca M, Bazan V, Macaluso M, Buscemi M, Gebbia N, Russo A (2003) STAT proteins: from normal control of cellular events to tumorigenesis. *J Cell Physiol* 197:157–168. doi:[10.1002/jcp.10364](https://doi.org/10.1002/jcp.10364)
45. Stephanou A (2009) JAK-STAT pathway in disease. Landes Bioscience, Austin
46. Rytinki MM, Kaikkonen S, Pehkonen P, Jääskeläinen T, Palvimo JJ (2009) PIAS proteins: pleiotropic interactors associated with SUMO. *Cell Mol Life Sci* 66:3029–3041. doi:[10.1007/s00018-009-0061-z](https://doi.org/10.1007/s00018-009-0061-z)
47. Schmidt D, Müller S (2003) PIAS/SUMO: new partners in transcriptional regulation. *Cell Mol Life Sci* 60:2561–2574. doi:[10.1007/s00018-003-3129-1](https://doi.org/10.1007/s00018-003-3129-1)
48. Larsen L, Ropke C (2002) Suppressors of cytokine signalling: SOCS. *Apmis* 110:833–844. doi:[10.1034/j.1600-0463.2002.1101201.x](https://doi.org/10.1034/j.1600-0463.2002.1101201.x)
49. Sen B, Peng S, Woods DM, Wistuba I, Bell D, El-Nagar A, Lai SY, Johnson FM (2012) STAT5A-mediated SOCS2 expression regulates Jak2 and STAT3 activity following c-Src inhibition in head and neck squamous carcinoma. *Clin Cancer Res* 18:127–139. doi:[10.1158/1078-0432.CCR-11-1889](https://doi.org/10.1158/1078-0432.CCR-11-1889)
50. Basham B, Sathe M, Grein J, McClanahan T, D'Andrea A, Lees E, Rascle A (2008) In vivo identification of novel STAT5 target genes. *Nucleic Acids Res* 36:3802–3818. doi:[10.1093/nar/gkn271](https://doi.org/10.1093/nar/gkn271)
51. Richard AJ, Stephens JM (2011) Emerging roles of JAK-STAT signaling pathways in adipocytes. *Trends Endocrinol Metab* 22:325–332. doi:[10.1016/j.tem.2011.03.007](https://doi.org/10.1016/j.tem.2011.03.007)